Article

Atomic Investigation on Cold Deformation Behavior of Two Phase TiAl Polycrystalline with and without Void Defect

Author

[1] School of Mechanical and Electronical Engineering, Lanzhou University of Technology, Lanzhou 730050, China;
[2] State Key Laboratory of Advanced Processing and Recycling of Non-ferrous Metals, Lanzhou University of Technology, Lanzhou 730050, China
* Correspondence: e-mail@e-mail.com; Tel.: +x-xxx-xxx-xxxx

Version November 1, 2018 submitted to Metals

Abstract: Cold deformation behavior of polycrystalline metallic materia is affected by dislocation, nano void and other defects. Existing studies on two phase TiAl alloy covers about deformation behavior mainly on marco scale. This paper mainly concern about cold deforamtion mechanism of the two phase TiAl ally at atomic scale, and the role of void defect in deformation process. Molecular dynamics simulation was performed to study the evolution of a spherical nano void in α_2+γ two-phase titanium-aluminium alloy under uniaxial tension. Simulation cases of model with different size and position of void were performed. The results show that i) γ phase is the major deformation source of the two phase alloy; ii) Voids defect detracts the strength of the two phase alloy, however the position of void affect the degree of this substraction: voids located at the α_2/γ phase boundary have significant detract to strength.

Keywords: two phase TiAl alloy; void; molecular dynamics

1. Introduction

Poor Ductility at room temperature in Ti-Al alloy strongly affects the safety of fracture of structure like turbo of aircraft engine and combustion generator [1]. Deformation phenomena of TiAl alloys have been widely studied in order to overcome the problems associated with the limited ductility and damage tolerance. Much of the work has been performed on single phase γ alloys and PST crystals[2]. Rapture failure at the macroscopic scale can be attributed to nucleation, growth and propagation of cracks, but at the microscopic scale cracks are initially easily formed at defects in the casting process, such as voids and inclusions [3]. The initiation of crack at microscopic scale is a dynamic process, which resulting in difficulties on study of detailed mechanisms of deformation and cracking. These defects are known to play a fundamental role in the deformation of the material. It has been known that nucleation, growth and coalescence of voids are deemed as the primary mechanism of ductile material fracture, in which void growth is particularly important [4]. Therefore, it is necessary to study the deformation response of intermetallic structural materials with the consideration of microstructure evolution.

A great number of literature covers a wide range of parameters such as alloy composition, microstructure and deformation temperature. Two-phase titanium aluminum alloys with proper phase distribution and grain size exhibit better mechanical performance compared with monolithic constituents γ(TiAl) and γ(Ti_3Al) alloy [5]. Due to difficulties in observing the dynamic process during deformation wit expeiments, MD simulation has become a effective method to investigate micro deformation mechanism. Defects such as grain boundary, void and segregation plays an significant role in the process of fracture [6]. In order to understanding the mechanism of brittle fracture, multi-scale methods from micro to marco scale have been applied to investigate the behavior of fracture. It's necessary to carefully examine the revolution of defects and its influence on the fracture process at atomic scale. The effect of void defect is another great concern about properties of deformation mechanism about of TiAl alloy. A previous study on void growth in γ-TiAl single crystal has reveals that void with high volume fraction detracts yield strength, and emission of dislocation [3,7]. Evolution of void in ductile polycrystalline was studied in nanoscale with MD simulations. [8,9]. The deformation and fracture mechanisms in the duplex microstructure are plasticity induced grain boundary decohesion and cleavage, while those in the lamellar micro-structure are interface delamination and cracking across the lamellar [3]. It has reveals that existence of voids alone may contribute to strain hardening because theyare barriers to dislocation movement [10].

However, few literatures covers about deformation mechanism of two phase TiAl alloy and the role of void in atomic scale. This paper focus on the evolution of microstructure, tend to find out the connection between microstructure and cold deformation behaviour of two phase TiAl alloy. MD simulaiton including model creation and analysis method is given in Section 2; Results and discussion are in Section 3.

2. Molecular Dynamics Simulation

2.1. Atomic Potential

The interaction of particle in the material is determined by interatomic potential. Many reported examples of crack propagation in metal materials were performed with embedded atomic method due to is better accuracy in metal lattice compare with F-S and L/J [11]. The embedded atom method (MEAM) potential developed by Zope and Mishin [12] was used in the study. The simulation is submitted by MD simulations with the Large-scale Atomic/Molecular Massively Parallel Simulator (LAMMPS) open-source code [13]. We performed constant-pressure and constant-temperature (NPT) molecular dynamics simulation. The definition of potential is as following:

$$E_{total} = \sum F_i(\rho_{h,i}) + \frac{1}{2}\sum_{i}\sum_{j(\neq 1)} \phi_{ij}(R_{ij}) \tag{1}$$

where E_{total} is the total energy of the system, $\rho_{h,i}$, is the host electron density at atom i due to the remaining atoms of the system,$F_i(\rho)$ is the energy for embedding atom i into the background electron density ρ, and $\phi_{ij}(R_{ij})$ is the core-core pair repulsion between atoms i and j separated by the distance R_{ij}. It can be noted that F_i only depends on the element of atom i and ϕ_{ij} only depends on the elements of atoms i and j. The electron density is, as stated above, approximated by the superposition of atomic densities.

2.2. Model Creation of Crystalline

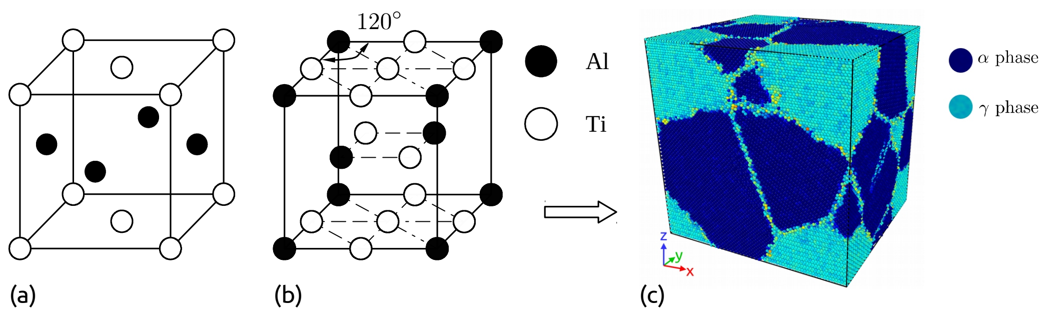

Figure 1. Unit cell of TiAl (a) and Ti_3Al (b)

Table 1. Parameters of nanocrystalline

Phase	Space group	Designation	Parameters
α_2 - Ti_3Al	$P6_3/mmc$	0_{19}	a = 0.5765
			c = 0.46833
γ - TiAl	tP4	$L1_0$	a = 0.3997
			c = 0.4062

γ TiAl has a fcc-centered tetragonal with an $L1_0$ structure, and $\alpha_2 - Ti_3Al$ has hcp structure, the two types of initial cells are shown in Fig. 1, and the constructing parameters are givin by Table 1. In order to study the deformation mechanism of the two phase alloy and the effect of void defect, three types of models were created: Type-1.model without any void defect; Type-2. models with different size void inside α_2 phase; Type-3. models with void at $\alpha_2 - \gamma$ interface. 1. The simulation cells of two phase polycrystalline with an initially spherical void at different position are shown in figure . Periodic boundary conditions (PBC) are applied along all three directions, that makes poly crystal with periodic nanovoid structures. The initial dimension of simulation cell is $L_x = 200$ Å, L_y =180Å, $L_z = 210$ Å, and each model contains about 4.6 million atoms. The grain orientation and size were randomly created with Voronoi method with code ATOMSK [14], and resulting in the arbitrary shape and orientation of the grains. Unixial load was applied to the model at a strain rate of 5×10^8 s^{-1}.

2.3. Analysis method

In order to identify typical defects in the deformed model, a hybrid analysis method was used with free code ovito[15].Dislocation is visualized by DXA method, and Centrossymmetry parameter(CSP) is used to tell grain boundary from α_2 phase and γ phase. The definition of CSP is as following:

$$P = \sum_{i=1}^{6} |\vec{R}_i + \vec{R}_{i+6}|^2 \tag{2}$$

where $\vec{R}_i$ and $\vec{R}_{i+6}$ are the vectors corresponding to the six pairs of opposite nearest neighbors in the fcc lattice. The centrosymmetry parameter(CSP) is zero for atoms in a perfect lattice. In other words, if the lattice is distorted the value of P will not be zero. Instead, the parameter will have a value within the range corresponding to a particular defect. By removing all the perfect and surface atoms within the bulk, the existence of dislocation atoms become visible.

3. Results and Discussion

Deformation process of the model witout void defect is shown in Fig. 2. The streng of the model without void defect is 5.3 Gpa. According to stress response under constan rate of strain rate, the whole tensile process can be divided into four stages: Stage - I: elasetic stage,ranging from $\epsilon = 0$ to $\epsilon = 0.092$, including key point 1; Stage - II: yield stage, ranging from $\epsilon = 0.092$ to $\epsilon = 0.101$, including key points 2 to 6; Stage - III: cracking stage, ranging from $\epsilon = 0.101$ to $\epsilon = 0.112$, including key pint 7 to 10; Stage - IV: fracture stage. Following discussion concentrates on deformation phenomena that rely on the elastoplastic co-deformation of the γ and α_2 phases and on the particular point defect situation occurring in two phase alloys.

Table 2. Key point during tensile process

Key Number	1	2	3	4	5	6	7	8	9	10
Stage	I	I	II	II	II	II	III	III	III	III
Strain	0.05	0.092	0.092	0.096	0.099	0.101	0.104	0.107	0.110	0.112

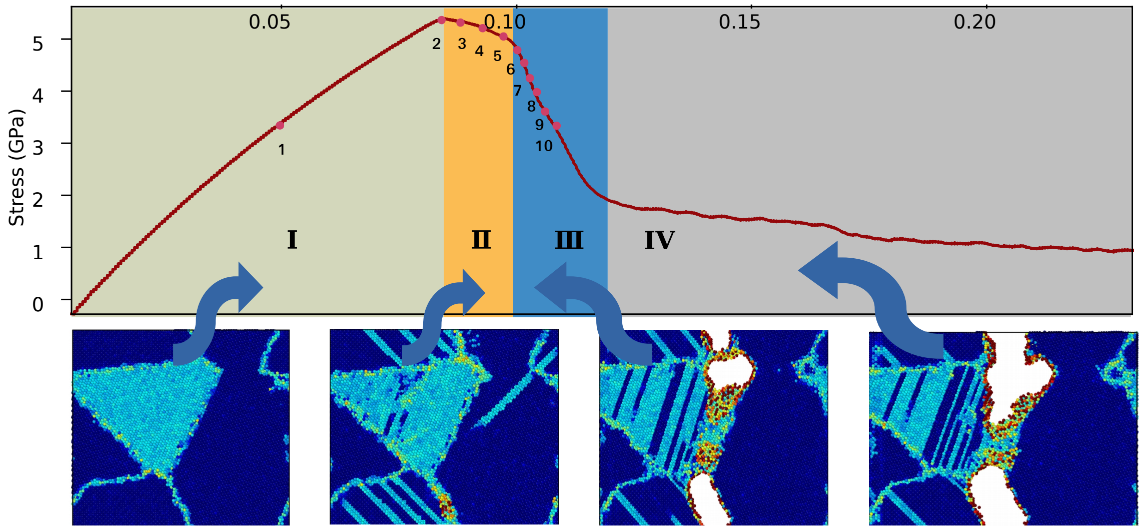

Figure 2. Deformation process of the model without void defect

3.1. Deformation Mechanism of Two Phase TiAl Alloy without Void Defects

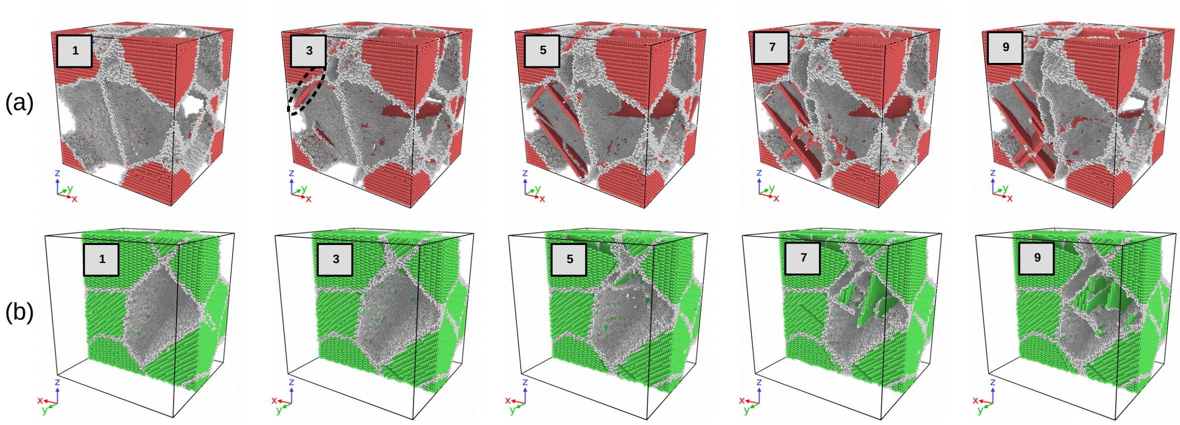

Figure 3. Microstrucutre evolution inside γ phase(a), α_2 phase(b) at key point 1 to 10

Deformation process of model without void under uniaxial load is shown by stress-strain curve Fig. 2 and snapshots of atom configuration at the 10 key points in Fig. 3. Atoms with ordered orientation of γ phase grains have been removed in Fig.3a, α_2 phase and defects inside grains have been left. Similarly, γ phase grain have been removed in Fig. 3b, the defect of α_2 phase has been left.

The results show that, at elastic stage(stageI), the structure of model have little change but the size of simulation box enlarged due to the loading, the deformation of the two phase are compatible. Emission of dislocation and evolution of defects initiated at the end of elastic stage (key point 2). A great number of dislocation emitted inside γ phase stage 2, however, the dislocation inside γ phase was emitted after key point 6 in Fig. 3b. The deformation of α_2 phase is even more earlier than γ phase druing yied stage, thus local displacement of two phase are incompatible during yield stage. γ phase (TiAl) deforms by octahedral glide of ordinary dislocations with the Burgers vector b=1/2[110] and super dislocations with the Burgers vectors $b = [101]$ and $b = 1/2[11\bar{2}]$. The other potential deformation mode is mechanical twinning have been repored along $1/6[11\bar{2}]111$, have not been observed in the simulation because of room temperature cannot offer enough energy for dislocation nucleation.

$$[\,0\,1\,\bar{1}\,] \rightarrow 1/2[\,1\,1\,\bar{2}\,] + 1/2[\,\bar{1}\,1\,0\,] \tag{3}$$

The velocity of a screw dislocation can be estimated by Escaig's elastic model [16], it can be written as

$$v = v_0 \exp(-\Delta H(\tau^*)/kT) \tag{4}$$

where the prefactor v_0 gives the velocity that would be obtained for each potential mobility, L is the free length of screw character of dislocation, $\Delta H(\tau^*)$ is activation enthalpy determined by loading conditions. The effect of temperature on the mobility can be obtained under different loading conditions, thus $\Delta H(\tau^*)$ are different. We choose cases with different loading condition$\Delta H(\tau^*)$, normalized velocity can be case 1 to case 3 in a increse order of $\Delta H(\tau^*)$. t

The orientation of slip is changed because the crystallographically available slip and directions are not continuous across the interface. This may significantly reduce the Schmid factor and thus impede slip transfer. At the γ/γ interfaces the orientation of the slip plan could change through a relevantly large angle of about 90 degree. Reorientation of slip is always required at the α_2/γ interface; the smallest angle between the corresponding slip planes 111_γ and $10-10_{\alpha_2}$ is about 19 degree []. From Fig. 3, of the two constituents of (α_2+γ) alloys, the α_2 phase is more difficult to deform. A reason for the unequal strain partitioning between the α_2 and γ phase is certainly the strong plastic anisotropy of the α_2 phase. TEM examinations performed on tensile tested lamellar alloys have revealed that the limited plasticity of the α_2 phase is mainly carried by local slip of [a]-type dislocations with the Burgers vector $b = 1/3[11\bar{2}0]$ prism planes3, which is by far the easiest slip system in α_2 single crystals.

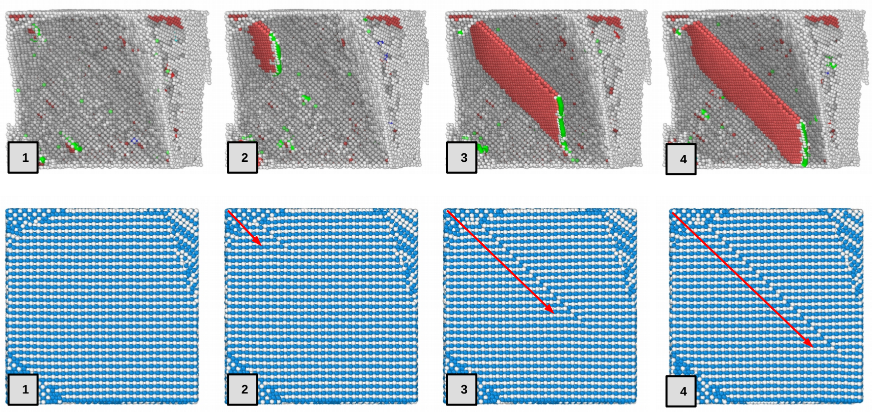

Figure 4. Dislocation in γ

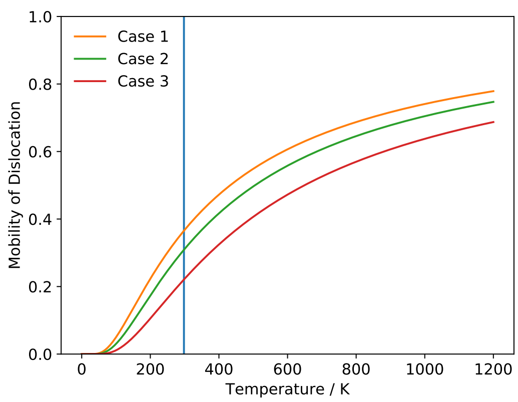

Figure 5. Mobility of dislocation

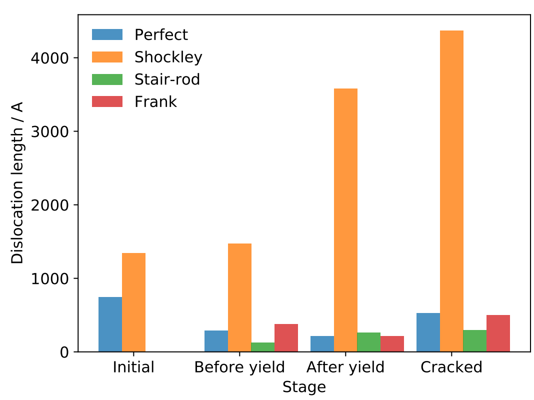

Figure 6. Strength of models

The core of a dislocation intersecting an interface often needs to be transformed. For example, an ordinary 1/2[110] dislocation gliding in one γ grain has to be converted in to a [101] super dislocation with the double Burgers vector gliding in an adjacent γ grain. At the α_2/γ interface the dislocations existing in the $D0_{19}$ structure have to be transformed into dislocations consistent with the $L1_0$structure. These core transformations are associated with a change of the dislocation line energy because the lengths of the Burgers vectors and the shear module are different.

Dislocations crossing semi-coherent boundaries have to intersect the misfit dislocations, a process that involves elastic interaction, jog formation and the incorporation of gliding dislocations into the mismatch structure of the interface.When the slip is forced to cross α_2 lamealla, pyramidal slip of the α_2 phase is required, which needs an extremely high shear stress.

3.2. The effect of void on the strength of material

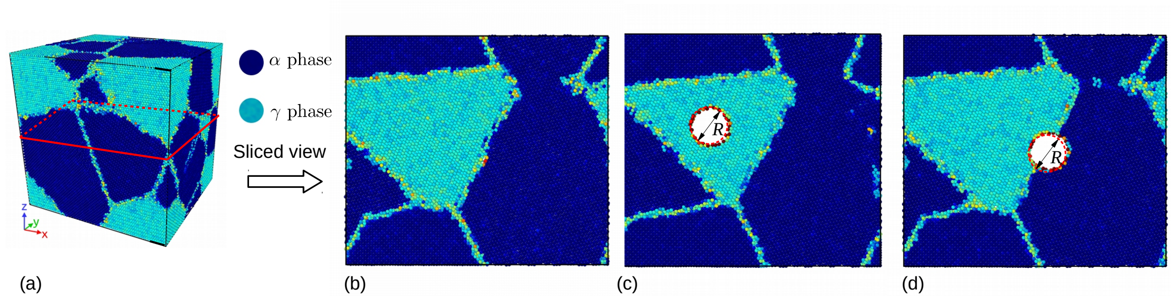

Figure 7. Model with no void defect (b), with void inside α_2 phase (c) with void at $\alpha_2 - \gamma$ interface (d)

Void of R=10 Å was placed at phase boundary, inside α_2 phase grain respectively. Effect of void at different position under uniaxial tension is shown in Fig.8. The strength of materails with void in different size and at different position is shown in Fig.8. The results show that the model without void defect has best strength, while the void located inside α_2 phase detracts the strength of the material most, and the void at phase boundary have less impact on the strength.

The effect of size is expectable that the greater voids detracts the strength of the materials more, however, it has been observed in the simulation that there is a critical value about 15A for voids at different position. The voids larger than 15 A have dramatic detraction to the strength of the material. Conventional definition of strength of materials with geometry subtraction was applied to the model, and theoretical strength of the models was calculated by formulation 5:

$$\sigma^* = \sigma_0 \cdot \frac{A^*}{A_0} \tag{5}$$

where σ_0 is the strength of the model without void defects 5.26 Gpa, and A_0 is initial section area, $A = 36000AA^2$, A^* is section area in consider of the subsection that results from the voids. Comparing with the strength determined by molecular dynamics simulation and the results calculated with formulation 5, it can be assumed that the main factor that affects the strength of materials can be attributed to local behaviour of the materials, thus revolution of defects should be examined carefully.

Voids with different size: 2A, 5A, 10A, 15A were placed into the model respectively. It has been observed that voids detracts the strengths of the material. The max stress stress of the simulation cell decreases as the volume of voids are lareger. From Fig 8, there is a critical value of void radius about 15A, the void greater than 15A cause serious detraction of strength of material. Engineering stress is calculated

$$\sigma = S/A$$

The rate of decrease of loading area are smaller comparing with the detraction of strength, so it can be assumed that the yield yield behavior and strength is much more related with local behaviour of grain boundaries and void.

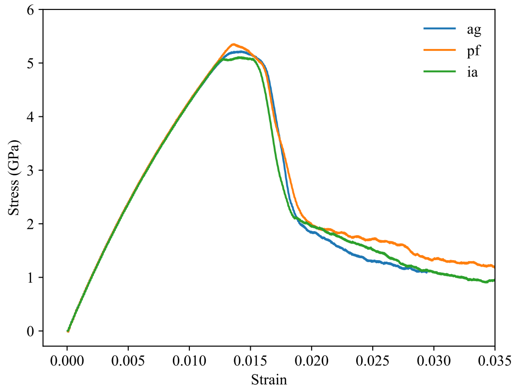

Figure 8. Stress-Strain

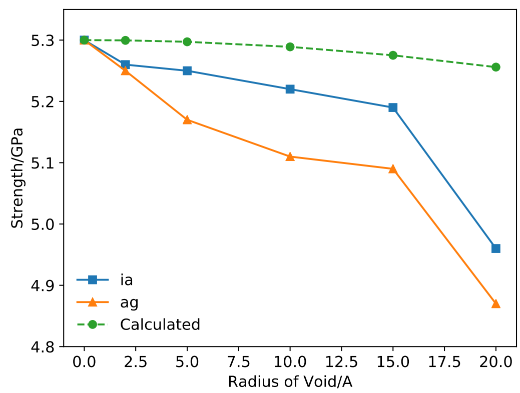

Figure 9. Strength of models

Grain and phase boundaris are obstancles to deformation process, thus the stability of boundaries have great impact on the strength of materials. Interactive between grainboundary and void determins the fracture mode of the TiAl alloy.

3.3. Evolution of spherical void in the simulation with intragranular spherical voids

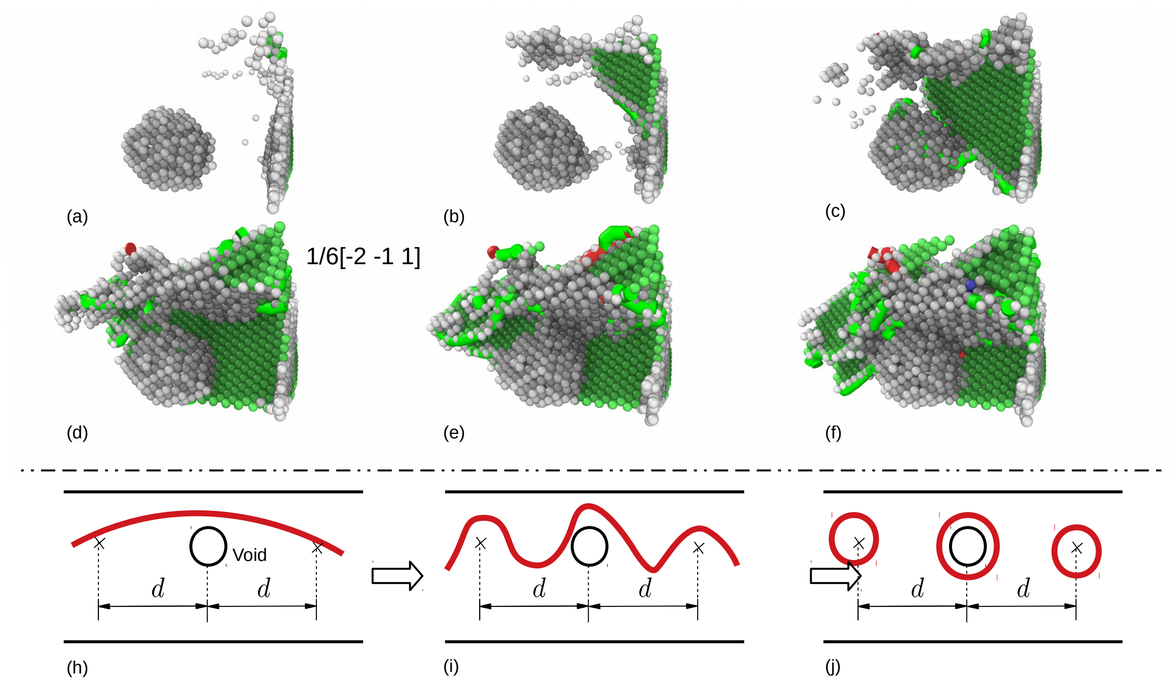

Figure 10. Orowan process in α-phase (α phase atoms have been removed)

The role of void can be concluded as two main parts: source of dislocation and obstacles to dislocations. Second-phase particles, precipitated within, as a consequence of a thermal treatment, or taken up, as a consequence of a material processing route, into a matrix of the first, dominant phase, disrupt, more or less (as possibly associated with the occurrence of incoherent or coherent interfaces;the long-range translation symmetry of the matrix. They may induce considerable misfit-stress fields and thus can influence material properties pronouncedly. Such stress fields surrounding the second-phase particles can be due to misfit between the volume occupied by the second-phase particle when unconstrained and the space ("hole") put at its disposal by the matrix. Such misfit can arise due to specific volume differences induced by precipitation or by different thermal expansion or shrinkage upon heating or cooling the specimen. A possibly favorable effect of second-phase particles is a contribution to the enhancement of mechanical strength. Considering yielding of a material as related to glide of dislocations, any mechanism obstructing dislocation glide improves the mechanical strength. In the discussion of the Frank–Read source for dislocation (-line) production it was made clear that second-phase particles can serve as obstacles for dislocation migration: the stress fields surrounding the second-phase particles can be of "antagonistic" nature and "block" propagation of the stress field of a migrating dislocation: the second-phase particle acts as "pinning point". It was already indicated that in order that a dislocation can pass two pinning points a critical shear stress is needed that depends on the distance between the obstacles (which can be second-phase particles):

$$\tau_0 = Gb/d \tag{6}$$

where d represents the distance between A and B and thus reflects the dependence of the critical shear stress τ_0 on the second-phase particle density and distribution. This mechanism for hardening is designated as the Orowan process (with τ_0 as the Orowan (shear) stress. As a result of the Orowan process, upon passage of the pinning points by a series of gliding dislocations, a system of concentric loops is formed around the second-phase particles. Consequently, the effective average distance between the second-phase particles has decreased to d which implies a necessary increase of the value of critical shear stress required for continuation of dislocation glide. The width of a burgers vector, will be generated at both sidesof a crystal along the direction of the burgers vector after dislocation traversing the entire crystal, as is shown in 10. A small tep will be formed at spherical void surface toward the void interiorafter dislocation absorption at spherical void surfaces. If a great number of dislocation slip along their respective systemstowards the spherical nano void in all directions, and are absorbed at fhe spherical void surfaces, the spherical nano void will eventually shrink from the dash circle

4. conclusion

In this paper, annealing processes of γ-TiAl alloy after introducing residual stress into prepressing are simulated, and the dynamic evolution process of microdefects and the distribution of residual stress before and after annealing are investigated. The conclusions are as follows:

(1)

(2) .

References

1. Munz, E.D. Psychotherapie in der Psychiatrie. *Nervenheilkunde* **2017**, *36*, 800–805, [arXiv:1011.1669v3]. doi:10.1007/s13398-014-0173-7.2.
2. Appel, F.; Clemens, H.; Fischer, F.D. Modeling concepts for intermetallic titanium aluminides. *Progress in Materials Science* **2016**, *81*, 55–124. doi:10.1016/j.pmatsci.2016.01.001.
3. Xu, X.T.; Tang, F.L.; Xue, H.T.; Yu, W.Y.; Zhu, L.; Rui, Z.Y. Molecular dynamics simulations of void shrinkage in γ-TiAl single crystal. *Computational Materials Science* **2015**, *107*, 58–65. doi:10.1016/j.commatsci.2015.05.007.
4. Hempel, N.; Bunn, J.R.; Nitschke-Pagel, T.; Payzant, E.A.; Dilger, K. Study on the residual stress relaxation in girth-welded steel pipes under bending load using diffraction methods. *Materials Science and Engineering A* **2017**, *688*, 289–300. doi:10.1016/j.msea.2017.02.005.
5. Kim, Y.W. Effects of microstructure on the deformation and fracture of γ-TiAl alloys. *Materials Science and Engineering: A* **1995**, *192-193*, 519–533. doi:10.1016/0921-5093(94)03271-8.
6. Larsen, P.M.; Schmidt, J. Robust structural identification via polyhedral template matching. *Modelling and Simulation in Materials Science and Engineering* **2016**, *24*, 055007, [1603.05143]. doi:10.1088/0965-0393/24/5/055007.

7. Xu, X.T.; Tang, F.L.; Xue, H.T.; Yu, W.Y.; Zhu, L.; Rui, Z.Y. Molecular dynamics simulations of void shrinkage in γ-TiAl single crystal. *Computational Materials Science* **2015**, *107*, 58–65. doi:10.1016/j.commatsci.2015.05.007.
8. Jing, P.; Yuan, L.; Shivpuri, R.; Xu, C.; Zhang, Y.; Shan, D.; Guo, B. Evolution of spherical nanovoids within copper polycrystals during plastic straining: Atomistic investigation. *International Journal of Plasticity* **2018**, *100*, 122–141. doi:10.1016/j.ijplas.2017.09.016.
9. Elkhateeb, M.G.; Shin, Y.C. Molecular dynamics-based cohesive zone representation of Ti6Al4V/TiC composite interface. *Materials and Design* **2018**, *155*, 161–169. doi:10.1016/j.matdes.2018.05.054.
10. Xiong, L.; Xu, S.; McDowell, D.L.; Chen, Y. Concurrent atomistic-continuum simulations of dislocation-void interactions in fcc crystals. *International Journal of Plasticity* **2015**, *65*, 33–42. doi:10.1016/j.ijplas.2014.08.002.
11. Ko, W.S.; Grabowski, B.; Neugebauer, J. Development and application of a Ni-Ti interatomic potential with high predictive accuracy of the martensitic phase transition. *Physical Review B* **2015**, *92*, 134107. doi:10.1103/PhysRevB.92.134107.
12. Zope, R.R.; Mishin, Y. Interatomic potentials for atomistic simulations of the Ti-Al system. *Physical Review B - Condensed Matter and Materials Physics* **2003**, *68*, 024102, [arXiv:cond-mat/0306298]. doi:10.1103/PhysRevB.68.024102.
13. Plimpton, S. Fast parallel algorithms for short-range molecular dynamics. *Journal of Computational Physics* **1995**, *117*, 1–19, [arXiv:10.1002/nag.2347]. doi:10.1006/jcph.1995.1039.
14. Hirel, P. Atomsk: A tool for manipulating and converting atomic data files. *Computer Physics Communications* **2015**, *197*, 212–219. doi:10.1016/j.cpc.2015.07.012.
15. Stukowski, A. Visualization and analysis of atomistic simulation data with OVITO-the Open Visualization Tool. *Modelling and Simulation in Materials Science and Engineering* **2010**, *18*, 015012, [arXiv:10.1002/nag.2347]. doi:10.1088/0965-0393/18/1/015012.
16. Escaig, B. L'activation thermique des déviations sous faibles contraintes dans les structures h.c. et c.c. Par. *Physica Status Solidi (b)* **1968**, *28*, 463–474. doi:10.1002/pssb.19680280203.

Funding: This research was funded by the National Natural Science Foundation of China (No. 51665030) and the Program for Changjiang Scholars and Innovative Research Team in Universities of the Ministry of Education of China (No. IRT-15R30) and the Doctoral Research Foundation of Lanzhou University of Technology.

mark